Comparison of Mean-Field Theory and ^{1}H NMR Transversal Relaxation of Poly(dimethylsiloxane) Networks

D. A. Vega, M. A. Villar, and E. M. Vallés*

Planta Piloto de Ingeniería Química, PLAPIQUI (UNS-CONICET), C.C. 717 (8000) Bahía Blanca, Argentina

C. A. Steren and G. A. Monti

Facultad de Matemática, Astronomía y Física, Universidad Nacional de Córdoba, Haya de la Torre y Medina Allende, Ciudad Universitaria (5000), Córdoba, Argentina

Received January 5, 2000; Revised Manuscript Received May 31, 2000

ABSTRACT: We have estimated the mass fraction of elastic and pendant chains of model poly(dimethylsiloxane) (PDMS) networks using transverse proton relaxation in nuclear magnetic resonance (^{1}H NMR). These experiments were compared with theoretical estimations of the mass fraction of pendant chains predicted by mean-field calculations (MFC). A recursive approach, originally postulated by Miller and Macosko and extended by the authors to obtain information on several molecular parameters related to the molecular structure of the pendant chains, was employed for the theoretical calculations. A preliminary inspection of the results showed that proton relaxation measurements underestimate the mass fraction of pendant material. We speculate that trapped entanglements, in which long pendant chains are involved, may act as temporary cross-linking points in the time scale of the ^{1}H NMR experiments. In this condition only portions of the pendant chains would be detectable by the experiments, justifying the observed differences between proton relaxation experiments and the MFC results. To verify this presumption, we formulated a modification of the recursive calculations to estimate the amount of entanglements in which pendant chains are involved. If entanglements are taken into consideration, a very good agreement between theoretical mass fraction of pendant chains calculated by the modified MFC and experimental values determined from proton relaxation is obtained.

Introduction

Polymer networks contain a complex structure characterized by the presence of elastically active chains, which are those chemically connected to the gel structure at their extremes. Other types of chains with different structure are also present in real networks. These chains are usually referred as part of the network defects. Free chains trapped in the network and pendant chains connected to the gel by one of their end units are the most common type of defects. The structure and concentration of these defects affect considerably the equilibrium and dynamic properties of networks.[1]

To study the influence of network defects on their properties, it is convenient to work with tailor-made systems that have a well-defined molecular structure. It is usually difficult to synthesize networks with controlled amounts of pendant chains of uniform length. Networks obtained by random cross-linking result in a broad molecular weight distribution of the elastic and pendant chains. This makes them not very suitably for studies aiming to reveal relationships between the structure of pendant chains and dynamic properties of polymer networks.

To obtain networks with controlled amounts of pendant chains with uniform length, we have prepared them by end-linking linear molecules having reactive groups in their ends. Using the end-linking technique and a mix of long linear PDMS chains with reactive groups in one or both extremes, it is possible to obtain networks with a controlled proportion of linear pendant chains of uniform size.[2]

* To whom correspondence should be addressed. e-mail: valles@plapiqui.edu.ar.

Standard analytical techniques that require dissolution of the polymer are not suitable to study the structure of polymer networks. However, nuclear magnetic resonance (NMR) can be used as a direct technique to obtain network information. In the field of NMR, different techniques have been used such as dipolar and quadrupolar interaction ^{2}H NMR,[3−5] NMR imaging,[6] and transverse proton relaxation ^{1}H NMR.[7] The last of these techniques is the simplest to accomplish since it does not require the use of labeled chains such as deuterated ones.

At temperatures well above the glass transition, T_g, the time and length scales of molecular movements of chains in a network are similar to those observed for liquids. However, topological constrains of the chains impose restrictions to molecular movements. Soluble and pendant chain motions are different from that of elastic chains, and ^{1}H NMR is sensitive to the different behaviors. Elastic chains are fixed to the network at both ends, providing an anisotropy of the fast motions of the chain segments. This anisotropy is detected as a solidlike behavior in the ^{1}H magnetization decay.

Taking advantage of the different behavior of elastic chains from that of the soluble and pendant chains, it is possible to determine the mass fraction of elastic material in the network using ^{1}H NMR. However, under suitable dynamic conditions, if the weight-average molecular weight of the soluble and pendant chains is higher than the weight-average molecular weight between entanglements, M_e, these topological interactions will behave like effective cross-links. For this reason, values of mass fraction of elastic chains determined from ^{1}H NMR will also include the portion of pendant and free chains that are entangled in the polymer network.

10.1021/ma0000172 CCC: $20.00
Published on Web 12/14/2000

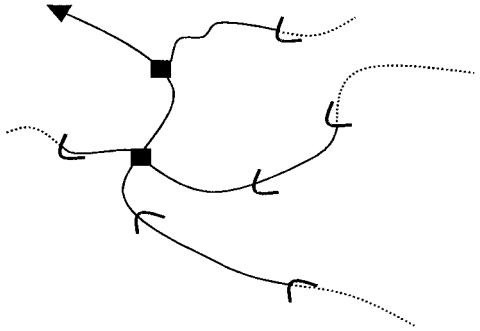

Figure 1. Schematic representation of a pendant chain. The arrow indicates the gel direction, and the filled squares represent cross-linking points. The solid lines show the entangled part of the chain, and the dotted lines correspond to the unentangled part.

In consequence, NMR measurements will overestimate the amount of elastic chains, and consequently the mass fraction of pendant and soluble chains will be miscalculated.

In this work we measured the transverse proton relaxation ^{1}H NMR of model poly(dimethylsiloxane) networks with controlled amounts of pendant chains. Previous to the NMR experiments the soluble fraction of the networks was extracted with an appropriate solvent. From those measurements, the mass fraction of elastic and pendant chains was obtained. The experimental values were finally compared with the predictions of the recursive calculations for the expected fraction of pendant chains.[8−10]

Theory

The basic ideas for the interpretation of the transverse proton relaxation in polymer networks are described in several publications.[11−16] The relaxation of the ^{1}H transverse magnetization is mainly determined by the dipole−dipole magnetic interaction between protons. This interaction is modulated at different extents by molecular motions, and therefore, it is sensitive to differences in the motion of the chains that form the polymer network. In the specific case of the dipolar interaction within a methyl group, due to the fast rotation of the protons around the c axis, the contribution of the dipolar interaction to the second moment (M_2) is reduced by a factor of 4. At the same time, the motion of the chain segments where the particular methyl group is attached also modulates the dipolar interaction.

In the context of NMR a polymer network at $T > T_g$ is a system formed by various mobile molecular parts which produce distinguishable relaxation signals. The main different molecular parts in an elastomeric network are (a) elastically active chains, (b) dangling or pendant chain ends, and (c) soluble molecules (see Figure 1).

The molecular motion of the polymer chain segments is fast and can be characterized by a correlation time $\tau_f \sim 10^{-8}$ s. These fast local motions may comprise methyl group reorientation, intra-Kuhn segments isomerization, and reorientation of the Kuhn segments by Rouse modes. Elastic chains are fixed at both ends, and this constraint induces an anisotropy in their fast motions. As a consequence, a small, mean residual part q ($q \sim 10^{-4}$) of the second moment of the dipolar interaction at rigid lattice remains. This residual part is further reduced by slower motions of the chain. These slower motions correspond to collective motions involving larger segments of the chain and can be characterized by a correlation time $\tau_s \sim 10^{-3}$ s. The mean residual qM_2 produces the solidlike behavior of the magnetization decay of the elastic chains. Similar behavior is expected for entangled chains, since the points of entanglement can be thought as fixed points within the NMR time scale.

The dangling or pendant chain ends are fixed to the network by one end, and therefore their motion is mainly isotropic. It has been reported in the literature that the ^{1}H transverse relaxation associated with these chains depends on the environment.[17,18] Particularly, for unfilled samples, it was found that the magnetization decay can be described by a single-exponential decay function. This behavior indicates a fast isotropic motion of the chain segment that average out the dipolar interaction ($q = 0$).

The magnetization of the soluble chains shows a behavior similar to that of the dangling chain ends. However, soluble molecules are not considered in the present analysis since they were extracted from the samples prior to the experiments.

For the analysis of the ^{1}H NMR experiments, it was assumed that the transverse magnetization decay in PDMS samples can be described as the sum of two contributions. These are the contribution of the elastically active chains on one hand and that of dangling chains on the other. The following equation can be used to describe the total transverse magnetization decay:

$$M_x(t) = W_E \exp\left[-\frac{t}{T_2} - qM_2\tau_s^2\left(\exp\left(-\frac{t}{\tau_s}\right) + \frac{t}{\tau_s} - 1\right)\right] + W_P \exp\left[-\frac{t}{T_2}\right] \quad (1)$$

where W_E and W_P are the contributions to the ^{1}H magnetization of the elastically active chains and dangling chains, respectively. The T_2 relaxation time is related to the fluctuating part of the Hamiltonian and corresponds to the homogeneous line broadening.[19] As we mentioned before, it is important to note that, at proper dynamic conditions, entanglements or topological interactions behave as cross-linking points and the chains between them as elastic ones contributing to W_E. For this reason only the unentangled part of the pendant chains will contribute to W_P.

Other approaches have been developed to describe the behavior of the elastic chains.[20,21] Sotta et al. have derived a model to describe the solidlike NMR behavior of elastomeric networks.[4] The authors use the isolated two-spin approximation. However, in PDMS samples, methyl groups are close enough to each other, making the two-spin approximation difficult to justify. Since our interest was mainly to quantify the mass fraction of elastic and pendant chains as observed by ^{1}H NMR, the functional form of eq 1 gives a suitable deconvolution in two components of the total magnetization $M_x(t)$.

Experimental Section

Model networks of PDMS were prepared by reacting long linear poly(dimethylsiloxane) chains with vinyl end groups, with tri- (A_3) or tetrafunctional (A_4) cross-linkers containing silane groups. Two types of linear chains were employed: a commercial difunctional prepolymer with vinyl groups at both extremes of the chains (α,ω-PDMS or B_2) and five nearly

Table 1. Molecular Characterization of the Linear Prepolymers Used for the Preparation of Model PDMS Networks

pre-polymer	M_n(FTIR) (Da)	M_n(GPC) (Da)	M_w(GPC) (Da)	M_w(LALLS) (Da)	M_w/M_n (GPC)
D_1		10 800	23 900		2.21
M_1	21 200	24 200	26 500	26 900	1.08
M_2	46 300	47 800	51 300	52 400	1.07
M_3	47 000	53 100	60 600	63 600	1.14
M_4	61 500	67 600	83 500	101 100	1.20
M_5	96 600	97 800	121 300	128 700	1.24

monodisperse monofunctional prepolymers with a vinyl group on one of the chain ends (ω-PDMS or B_1). The cross-linking process consists of a hydrosilylation reaction, based on the addition of the hydrogen from the silane reactive groups of the cross-linker to the α or ω vinyl end groups of the PDMS chains.

Known amounts of the B_2 chains and the monodisperse linear B_1 molecules were reacted with the trifunctional or tetrafunctional cross-linker in stoichiometric proportions. It has been shown that the final concentration of pendant chains in the network depends on the amount of B_1 chains added to the system and on the maximum extent of reaction that can be obtained for the working conditions.[10] Monofunctional B_1 chains constitute the basis of the pendant chains of the network at stoichiometrically balanced and completely reacted systems. However, if the reaction is not complete, additional chains of different structure will be also part of the pendant material.

Table 1 shows the results of the molecular weight characterization of the prepolymers. Difunctional prepolymer, D_1, was obtained from Dow Corning, and monofunctional molecules, labeled as M_1 to M_5, were synthesized by anionic polymerization using *n*-butyllithium as initiator and *n*-hexane as solvent.[22] Two cross-linkers were used: phenyltris(dimethylsiloxy)-silane (A_3) and tetrakis(dimethylsiloxy)silane (A_4) (United Chemical Technology Inc.). A Pt salt was employed as homogeneous catalyst for the reaction.

Table 2 shows the nomenclature and compositions of the networks analyzed. In this table f indicates the cross-linker functionality ($f = 3$ or $f = 4$), M_{wB_1} the weight-average molecular weight of monofunctional macromolecules, w_{B_1} the mass concentration of monofunctional chains B_1 added to the reaction, and r the stoichiometric imbalance (r = [A]/[B]). Reactants were weighted in order to obtain stoichiometrically balanced mixtures ($r = 1$) with different amounts of monofunctional chains. Reactive mixtures were mixed with a mechanical stirrer and degassed under vacuum to eliminate air bubbles. When trapped air was eliminated, the mixtures were placed between the parallel plates of a Rheometrics Mechanical spectrometer.

The cure reaction was carried out at 40 °C between the plates for 24 h. Viscoelastic properties were determined when the cure reaction was completed. All measurements were carried out in simple shear dynamic experiments with deformations up to 25%, within the range of linear viscoelastic response. The storage modulus $G'_{\omega\to 0}$ was obtained in the low-frequency limit (0.01 rad/s) at 40 °C and is reported in Table 2.

After viscoelastic measurements, networks were subjected to solvent extraction using toluene. Samples were weighted and placed in glass jars with solvent to remove the non-cross-linked polymer chains. The extraction of solubles was carried out at room temperature for about 1 month, and the solvent was replaced every 3 or 4 days. After the extraction, samples were dried under vacuum at 40 °C until complete removal of solvent was achieved. Dry samples were weighted again, and the mass fraction of solubles (w_S) was computed.

The maximum extent of reaction (α_{max}) was calculated from the experimental values of the mass fraction of solubles, w_S, using the recursive calculations. The results obtained for the different networks are shown in Table 2. More details on sample preparations, network structure, characterization, and dynamic properties can be found in previous works.[2,24,25]

The NMR experiments were carried out on a Bruker MSL-300 spectrometer at a resonance frequency of 300.13 MHz for protons. A DOTY DSI-703 proton dedicated probe with proton background signal reduction was used. Samples were packed in ZrO sample holders fitted with Kel-F end caps.

Transverse magnetization decays were measured by the common Hahn spin-echo pulse sequence $(\pi/2)-\tau/2-(\pi)-\tau/2-$ acquisition. The $\pi/2$ pulse duration was of 4 μs. The values of τ were varied in the range of 0.1−30 ms. The Hahn spin-echo sequence is used to refocuses the spin dephasing due to inhomogeneities from both the magnetic field and the chemical shift without influencing the interaction bilinear in the spin operators such as the dipolar interaction.

The phase cycling described by Turner[26] was implemented to eliminate the signals due to imperfections of the π pulse and the remnant FID due to the first pulse ($\pi/2$ pulse). All measurements were taken at a temperature of 29 ± 1 °C with a stability of 0.1 °C. The integral intensities obtained from the Fourier transform of the right half of the spin echoes were used as a measure of the proton transverse magnetization at a given time τ.

Figure 2 shows a characteristic transverse magnetization decay for one of the samples under study. A nonlinear least-squares fitting procedure was used to adjust the data to eq 1. W_E, $Q = qM_2$, τ_s, W_P, and T_2 were used as adjustable parameters. The values for T_2, τ_s, and w_P obtained from the analysis of the ^{1}H NMR data are displayed in Table 2; $w_P = W_P/(W_P + W_E)$ is the mass fraction of pendant chains. The solid line in Figure 2 corresponds to the values obtained using eq 1. The fast decay of the magnetization for $\tau \leq 5$ ms is assigned to the contribution of protons attached to the elastic and entangled chains (solidlike contribution). The slower decay of the magnetization for $\tau \geq 5$ ms is attributed to the contribution of the protons attached to the pendant chain ends.

It is important to note that the parameters W_P and T_2 are completely determined by the behavior of the magnetization decay at longer times, while W_E, Q, and τ_s are determined by the behavior of the magnetization for $\tau \leq 5$ ms. This can be visualized in Figure 2 where the contributions of the first and second term of eq 1 to the fit are shown.

Table 2. Nomenclature, Characteristics, and NMR Proton Relaxation Results from the PDMS Networks[a]

network	f	M_{wB_1} (Da)	w_{B_1} (wt %)	r	w_S (wt %)	α_{max}[b]	$G'_{\omega\to 0}$ (MPa)	T_2 (ms)	τ_s (ms)	w_P (wt %)
G0F300	3			1.002	0.6	0.937	0.214	6.7	2.0	11.1
G0F400	4			1.003	0.4	0.933	0.252	4.1	3.1	12.0
G1F320	3	26 700	0.202	1.013	4.9	0.906	0.120	6.1	5.0	32.2
G2F320	3	51 850	0.201	1.010	4.3	0.906	0.129	7.7	1.9	22.0
G3F320	3	62 100	0.199	1.053	4.1	0.880	0.147	8.0	1.9	18.8
G4F320	3	92 300	0.201	1.038	3.8	0.892	0.147	8.1	1.9	17.8
G5F320	3	125 000	0.199	1.026	3.9	0.896	0.144	7.5	2.0	18.2
G1F420	4	26 700	0.217	1.030	4.4	0.866	0.158	5.1	3.7	33.2
G2F420	4	51 850	0.203	1.015	5.1	0.854	0.154	6.1	1.7	24.7
G3F420	4	62 100	0.209	1.025	3.8	0.871	0.185	5.8	1.5	18.2
G4F420	4	92 300	0.214	1.036	3.0	0.878	0.182	5.5	1.6	17.9
G5F420	4	125 000	0.221	1.005	3.6	0.888	0.157	5.4	1.5	19.0

[a] $M_{wB_2} = 23\,900$ for all networks. [b] Calculated from values of soluble fraction (w_S).

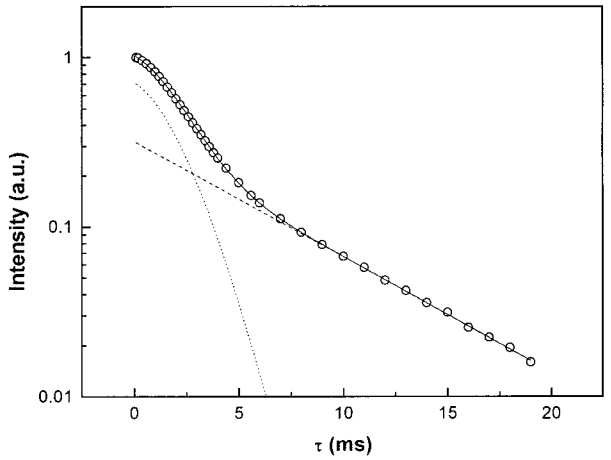

Figure 2. Total transverse magnetization decay (M_x) as a function of time. Sample G1F320, symbols correspond to experimental values and solid line to eq 1. The contributions of the first term, solidlike (· · ·), and the second term, liquidlike (- - -), of eq 1 are depicted separately.

Table 3. Molecular Weight between Cross-Linkings and Weight Fraction of Pendant Material for PDMS Networks Obtained from NMR[a] and Mean-Field Theory[b]

network	M_{wB_1} (Da)	M_c^b (Da)	w_P^a (wt %)	w_P^b (wt %)	$w_{P-B_2}^b$ (wt %)	$w_{P-B_1}^b$ (wt %)
G0F300		14 500	11.1 ± 1	14.5	11.7	
G0F400		11 500	12.0 ± 1	12.4	11.9	
G1F320	26 700	19 500	32.2 ± 1	40.1	12.6	18.0
G2F320	51 850	18 000	22.0 ± 1	38.6	13.1	18.1
G3F320	62 100	18 700	18.8 ± 1	36.9	12.2	18.0
G4F320	92 300	17 900	17.8 ± 1	36.4	12.1	18.3
G5F320	125 000	17 650	18.2 ± 1	36.7	12.9	18.0
G1F420	26 700	13 600	33.2 ± 1	38.4	15.4	19.7
G2F420	51 850	13 600	24.7 ± 1	40.3	18.9	18.0
G3F420	62 100	12 900	18.2 ± 1	36.8	15.5	19.1
G4F420	92 300	12 500	17.9 ± 1	34.6	13.2	19.8
G5F420	125 000	12 500	19.0 ± 1	37.1	15.3	20.2

Results and Discussion

The structure of pendant chains of networks obtained by end-linking difunctional chains (B_2) and a polyfunctional cross-linker (A_f) depends on the maximum extent of reaction reached by the system.

When the experimental maximum extent of reaction is close to unity, pendant chains are almost exclusively linear B_2 molecules connected to the networks by one end. On the other hand, at intermediate extents of reaction pendant chains may have branched complex structures.[10,25] Calculated values of the molecular weight between cross-linkings (M_c) and the mass fraction of pendant chains (w_P) are shown in Table 3.[10,25]

The values of mass fraction of pendant chains obtained from NMR experiments are always lower than the corresponding values calculated from the recursive approach (fourth and fifth columns of Table 3, respectively).

We believe that the cause of the observed difference is due to the fact that, at the frequencies normally used at ^{1}H NMR relaxation experiments, only the unentangled part of the pendant chains (dotted line in Figure 1) is detected. Under these conditions the entangled fraction of pendant chains (solid line in Figure 1) behaves as an elastic portion of the chains.

The networks analyzed were obtained using bifunctional molecules with a molecular weight similar to the entanglement molecular weight and monofunctional chains of different molecular weights. Then single B_2 chains reacted with the gel by one of the end-functional groups belong to the unentangled portion of pendant chains and are counted by NMR as pendant material. On the other hand, the entangled part of longer pendant chains also behaves as elastic chains.

In the case of networks G0F300 and G0F400 that do not contain monofunctional chains, it is possible to calculate the mass fraction of B_2 chains that both belong to the pendant material and have just one reacted end. This will account only for the fraction of B_2 chains on the terminal portion of the pendant chains. The mass fraction of B_2 chains which satisfy that condition ($w_{P-B_2}^b$) is given by the following expression:

$$w_{P-B_2}^b = 2w_{B_2}(1 - P(F_B^{out}))(1 - r\alpha) \qquad (2)$$

where w_{B_2} is the mass fraction of bifunctional chains in the reacting system, r the stoichiometric imbalance, α the extent of reaction, and $P(F_B^{out})$ the probability of finding a finite end going out from a B_2 chain randomly chosen in the recursive model.[8−10] Table 3 shows the values of $w_{P-B_2}^b$ obtained from eq 2. The values given by the model for the two networks prepared exclusively with B_2 chains are in very good agreement with those obtained by NMR.

The rest of the networks were prepared adding monofunctional chains (B_1) to the reaction system described before. In this case the length of monofunctional chains was changed in order to verify the influence of entanglements. All the monofunctional chains used have a molecular weight higher than the critical molecular weight between entanglements. For this reason, only the unentangled ends of the B_1 chains (dotted line of the molecule sketched in Figure 1) should be detected as pendant material by ^{1}H NMR relaxation experiments.

The weight fraction of monofunctional B_1 chains effectively jointed to the network, $w_{P-B_1}^b$, can be obtained by recursive calculations:[8−10]

$$w_{P-B_1}^b = w_{B_1}(1 - P(F_B^{out})) \qquad (3)$$

Values of $w_{P-B_1}^b$ obtained from eq 3 are also shown in Table 3. Comparing these values with the mass fraction of B_1 molecules added to the reacting system (fourth column in Table 2), we may conclude that more than 90% of the original monofunctional chains are effectively attached to the gel forming part of the pendant material.

If the NMR measurements disclose only the unentangled portion of the chains, the mass fraction of pendant chains observed by ^{1}H NMR relaxation experiments will be given by the pendant bifunctional molecules with only one end reacted plus the unentangled end of the monofunctional chains. This mass fraction of unentangled pendant chains is given by the following equation:

$$\hat{w}_P = w_{P-B_2}^b + \beta w_{P-B_1}^b \qquad (4)$$

where the constant β is inversely proportional to the molecular weight of the monofunctional chains:

$$\beta \propto \frac{1}{M_{wB_1}} \qquad (5)$$

Figures 3 and 4 show the values of mass fraction of pendant chains obtained from ^{1}H NMR relaxation

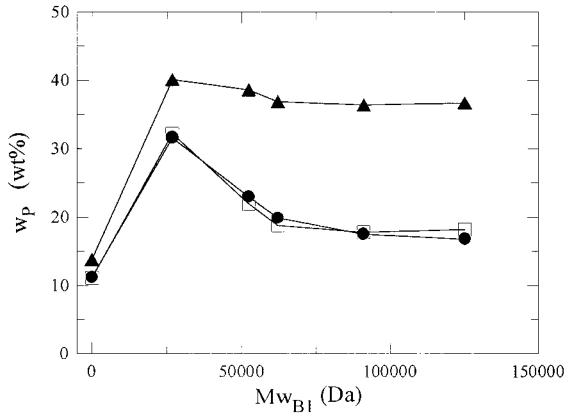

Figure 3. Mass fraction of pendant chains (w_P) as a function of weight-average molecular weight of monofunctional chains added (M_{wB_1}). Networks prepared with a trifunctional cross-linker ($f = 3$). Symbols: (□) ^{1}H NMR values, (▲) values predicted by mean-field theory (recursive approach), and (●) values calculated with eq 4 (recursive model taking into account the entanglements).

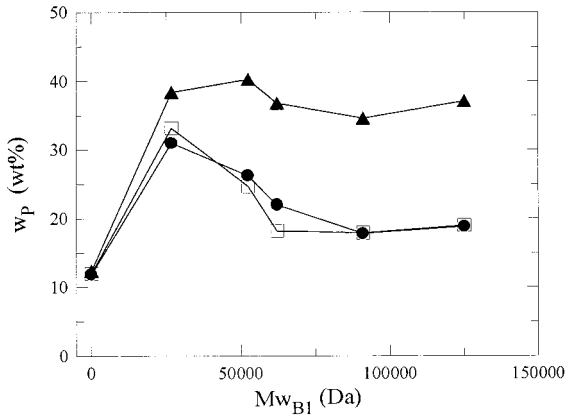

Figure 4. Mass fraction of pendant chains (w_P) as a function of weight-average molecular weight of monofunctional chains added (M_{wB_1}). Networks prepared with a tetrafunctional cross-linker ($f = 4$). Symbols: (□) ^{1}H NMR values, (▲) values predicted by mean-field theory (recursive approach), and (●) values calculated with eq 4 (recursive model taking into account the entanglements).

experiments, the corresponding values of the total mass fraction of pendant chains, and the unentangled mass fraction of pendant chains calculated from eq 4 as a function of the average molecular weight of the monofunctional chains (M_{wB_1}) added to the network. For comparison, networks without monofunctional chains, corresponding to $M_{wB_1} = 0$, were also included in the figures.

The mass fraction of pendant chains obtained by NMR is, in all cases, lower than the calculated values for the total mass fraction of pendant chains. The difference between both results is attributed to the entanglements in which pendant chains are involved. When the NMR results are compared with the theoretical calculations that take into account the presence of entanglements (eq 4), a very good agreement is found. In this case the constant of proportionality between the parameter β and the weight-average molecular weight of monofunctional chains (M_{wB_1}) was determined by least-squares fit. The value of the proportionality constant was found to be 28 000 g/mol for trifunctional networks and 21 000 g/mol for tetrafunctional ones.

The critical molecular weight between cross-linkings (M_e) for linear PDMS is on the order of 9000 g/mol.[27] As the critical molecular weight in order to obtain a temporary network in a dynamic measurement is between 2 and 3 times the M_e,[28] the values obtained for the adjusting parameter β are consistent with these result.

Conclusions

^{1}H NMR relaxation experiments have been shown to be a powerful technique to obtain the mass fraction of pendant material in rubber networks provided its molecular weight is lower than molecular weight between entanglements. When the molecular weight of dangling chains is higher than molecular weight between entanglements, the values of mass fraction of pendant material obtained from NMR measurements must be more carefully analyzed since only the unentangled part of these molecules is detected by this technique.

Estimation of the unentangled mass fraction of pendant material by recursive calculations is in very good agreement with NMR results. This accordance confirms the capability of the mean-field calculations to predict network molecular parameters.

Acknowledgment. We express our gratitude to the Consejo Nacional de Investigaciones Científicas y Técnicas (CONICET), the Agencia Nacional de Promoción Científica y Técnica (ANPCyT), the Secretaría de Ciencia y Técnica of the Universidad Nacional del Sur (UNS) and the Universidad Nacional de Cordoba (SECYT-UNC), the Consejo de Investigaciones Científicas y Técnicas de la Provincia de Córdoba (CONICOR), and the Fundación Antorchas which supported this work.

References and Notes

(1) Stepto, R. *Polymer Networks. Principles of their Formation, Structure and Properties*; Chapman & Hall: Bristol, U.K., 1997.
(2) Villar, M. A.; Vallés, E. M. *Macromolecules* **1996**, *29*, 4081.
(3) Brereton, M. G. *Macromolecules* **1990**, *23*, 1119.
(4) Sotta, P.; Fülber, C.; Demco, D. E.; Blümich, B.; Spiess, H. W. *Macromolecules* **1996**, *29*, 6222.
(5) McLoughlin, K.; Szeto, C.; Duncan, T. M.; Cohen, C. *Macromolecules* **1996**, *29*, 5475.
(6) Barth, P.; Hafner, S.; Denner, P. *Macromolecules* **1996**, *29*, 1655.
(7) Simon, G.; Baumann, K.; Gronski, W. *Macromolecules* **1992**, *25*, 3624.
(8) Miller, D. R.; Macosko, C. W. *Macromolecules* **1976**, *9*, 206.
(9) Miller, D. R.; Vallés E. M.; Macosko, C. W. *Polym. Eng. Sci.* **1979**, *19*, 272.
(10) Villar, M. A.; Bibbó, M. A.; Vallés, E. M. *Macromolecules* **1996**, *29*, 4072.
(11) Fedotov, V. D.; Tshernov, V. M.; Khasanovitsh, T. N. *Vysokomol. Soedin. A* **1978**, XX, *4*, 919. The English version of this journal is entitled *Polym. Sci. USSR*.
(12) Gotlib, Y. Y.; Lifshitz, M. I.; Shevelev, V. A.; Lishanskij, I. S.; Balanina, I. V. *Vysokomol. Soedin. A* **1976**, XXVIII, *10*, 2299. The English version of this journal is entitled *Polym. Sci. USSR*.
(13) Doscocilova, D.; Schneider, B. *Pure. Appl. Chem.* **1981**, *54*, 575.
(14) English, A. D. *Macromolecules* **1985**, *18*, 178.
(15) Simon, G.; Birnstil, A.; Schimmel, K. H. *Polym. Bull.* **1989**, *21*, 235.
(16) Brereton, M. G.; Ries, M. E. *Macromolecules* **1996**, *29*, 2644.
(17) Cohen-Addad, J. P.; Domard, M.; Hers, J. *J. Chem. Phys.* **1982**, *76*, 2744.
(18) Leisen, J.; Breidt, J.; Kelm, J. *Rubber Chem. Technol.* **1999**, *72*, 1.
(19) Abragam, A. *The Principles of Nuclear Magnetism*; Clarendon Press: Oxford, U.K., 1961.
(20) Cohen Addad, J. P. *J. Chem. Phys.* **1976**, *64*, 3438.
(21) Cohen Addad, J. P.; Dupeyre, R. *Polymer* **1983**, *24*, 400.

(22) Villar, M. A.; Bibbó, M. A.; Vallés, E. M. *J. Macrom. Sci., Pure Appl. Chem.* **1992**, *A29*, 391.
(23) Vallés, E. M.; Macosko, C. W. *Macromolecules* **1979**, *12*, 673.
(24) Villar, M. A. Ph.D. Thesis, Universidad Nacional del Sur, Bahía Blanca, Argentina, 1991.
(25) Vega, D. A. Ph.D. Thesis, Universidad Nacional del Sur, Bahía Blanca, Argentina, 1999.
(26) Turner, D. L. *Prog. NMR Spectrosc.* **1985**, *17*, 281.
(27) Ferry, P. *Viscoelastic Properties of Polymers*; John Wiley & Sons: New York, 1980.
(28) Doi, M. *Introduction to Polymer Physics*; Oxford University Press: Oxford, U.K., 1996.

MA0000172